



Contents lists available at ScienceDirect

Journal of Biomechanics

journal homepage: www.elsevier.com/locate/jbiomech
www.JBiomech.com

Biomechanical characterization of a chronic type a dissected human aorta



Marco Amabili^{a,b,c,*}, Goffredo O. Arena^{d,e}, Prabakaran Balasubramanian^a, Ivan D. Breslavsky^a, Raymond Cartier^f, Giovanni Ferrari^a, Gerhard A. Holzapfel^{g,h}, Ali Kassabⁱ, Rosaire Mongrain^{a,b}

^a Department of Mechanical Engineering, McGill University, Montreal H3A 0C3, Canada

^b Department of Biomedical Engineering, McGill University, Montreal H3A 2B4, Canada

^c Dipartimento di Ingegneria e Architettura, University of Parma, Parma, Italy

^d Department of Surgery, McGill University, St. Mary Hospital, Montréal H3T 1M5, Canada

^e Fondazione G. Giglio, Cefalù, Italy

^f Department of Cardiac Surgery, Montreal Heart Institute, Montréal HIT 1C8, Canada

^g Institute of Biomechanics, Graz University of Technology, Austria

^h Department of Structural Engineering, Norwegian University of Science and Technology Trondheim, Norway

ⁱ Research Center, Centre Hospitalier Universitaire de Montréal (CHUM) Université de Montréal, Montréal H2X 0A9, Canada

ARTICLE INFO

Article history:

Accepted 29 July 2020

Keywords:

Aortic dissection
Chronic dissection
Mechanical characterization
Viscoelastic material
Hyperelastic material

ABSTRACT

Aortic dissection is one of the most lethal cardiovascular diseases. A chronic Type A (Stanford) dissected aorta was retrieved for research from a 73-year-old male donor without diagnosed genetic disease. The aorta presented a dissection over the full length, and it reached a diameter of 7.7 cm in its ascending portion. The descending thoracic aorta underwent layer-specific quasi-static and dynamic mechanical characterizations after layer separation. Mechanical tests showed a physiological (healthy) behavior of the intima and some mechanical anomalies of the media and the adventitia. In particular, the static stiffness of both these layers at smaller strains was three times smaller than any one measured for twelve healthy aortas. When the viscoelastic properties were tested, adventitia presented a larger relative increase of the dynamic stiffness at 3 Hz with respect to most of the healthy aortas. The loss factor of the adventitia, which is associated with dissipation, was at the lower limit of those measured for healthy aortas. It seems reasonable to attribute these anomalies of the mechanical properties exhibited by the media and the adventitia to the severe remodeling secondary to the chronic nature of the dissection. However, it cannot be excluded that some of the mechanical anomalies were present before remodeling.

© 2020 Elsevier Ltd. All rights reserved.

1. Introduction

Aortic dissection typically starts with an intimal tear of the wall, followed by a crack in the radial direction. The crack then proceeds within the medial layer, or between the media and the adventitia, causing the layers of the wall to separate and creating a false lumen where the blood can flow into. This may reduce the blood flow to any of the arteries towards the periphery. Any disease that weakens the strength of the aortic wall may lead to aortic dissection (Erbel et al., 2001). The first few centimeters of the ascending aorta are the most common site for the initial rupture (Evangelista et al., 2018). Risk factors associated with aortic dissections include:

hypertension, age, atherosclerosis, connective tissue disorders such as Marfan syndrome and Ehlers-Danlos syndrome, infection, inflammation and blunt trauma (Erbel et al., 2001; Evangelista et al., 2018). Associations between mutations in smooth muscle α -actin and dissection have also been documented (Guo et al., 2007).

Aortic dissection can be acute or chronic. Stanford Type A aortic dissections are life-threatening emergencies in the acute phase that require immediate surgical repair for the high propensity to quickly develop severe complications, including aortic rupture, severe aortic regurgitation, pericardial tamponade, and cerebral and coronary malperfusion. Mortality estimates suggest that 20% of cases of Type A acute aortic dissection die before reaching the hospital (Erbel et al., 2001). There is about 1% mortality per hour within the first 48 h upon arrival (Erbel et al., 2001), and postoperative survival at 1 year postdischarge after surgical repair is evaluated at 96.1% (Evangelista et al., 2018). According to other data,

* Corresponding author at: Department of Mechanical Engineering, McGill University, Macdonald Engineering Building, 817 Sherbrooke Street West, Montreal, PQ H3A 0C3, Canada.

E-mail address: marco.amabili@mcgill.ca (M. Amabili).

overall in-hospital mortality was found to be 26% in case of surgical treatment and 58% for patients not receiving surgery (Hagan et al., 2000). In the last 20 years surgical repair mortality has reduced due to improvement in surgical techniques and resuscitative measures (Evangelista et al., 2018).

Chronic Type A dissection (CTAD) affects a subset of patients who were not diagnosed of the acute dissection for absence of typical symptoms. CTAD are considered to be present if more than 14 days have elapsed from the acute event and patients typically remain clinically and hemodynamically stable (Erbel et al., 2001). A more recent classification proposal considers CTAD if more than 30 days have elapsed (Evangelista et al., 2018). A relatively small number of Type A acute aortic dissection advance to the chronic phase due to the high mortality of patients not receiving surgery during the acute phase.

The underlying mechanisms of aortic dissection are also not yet fully understood. A review of the state-of-the-art in regard to experimental and numerical approaches aimed to study the mechanics of aortic dissections was presented in Tong et al. (2016). A review on the biomechanics of the ascending thoracic aorta is provided in Emmott et al. (2016) and Sherifova and Holzapfel (2019). In the study of Sommer et al. (2008), direct tension and peeling tests were performed on the media obtained from healthy abdominal aortas in order to clarify the mechanisms of dissection propagation. Some studies investigated the mechanical properties of diseased aortic tissues. Dissection properties of non-aneurysmal and aneurysmal human ascending thoracic aorta were identified in Pasta et al. (2012, 2016), while mechanical properties of the media of twelve aneurysmal and four dissected human thoracic aortas (14 ascending and 2 descending aortas) were investigated in Sommer et al. (2016) – tissues were obtained from patients undergoing surgical repair. Mechanical characterization of strips harvested from ascending aortas of twelve patients undergoing emergent surgical repair for type A dissection was performed in Manopoulos et al. (2018). Dissection properties of aneurysmal ascending thoracic aortas were investigated by Angouras et al. (2019). Refined models for aortic dissection were presented in Pal et al. (2014), Bellini et al. (2017), Thunes et al. (2018), Ahmadzadeh et al. (2019) and Gültekin et al. (2019). The identification of static and viscoelastic material parameters from healthy descending thoracic aortas (Amabili et al., 2019a, 2019b, 2020) is also useful in order to compare these data to those obtained from dissected aortas, which allows to identify mechanical anomalies.

Additional data on the mechanical properties of dissected aortas are of pressing need to advance studies and model validations. Aortic tissues tested in Sommer et al. (2016) and Manopoulos et al. (2018) were obtained from patients undergoing surgical repair. It seems that up to now no data on the layer-specific mechanical properties are available for a chronic Type A aortic dissection, which to identify is the goal of the present study. These properties are compared to those of the same segment of healthy aortas in order to better understand if mechanical anomalies are associated to the disease.

2. Case presentation

A 73-year-old male (weight 63 kg, height 154 cm) was brought by ambulance to the emergency department after having fallen unconscious to the floor. Initial Glasgow Coma Score of 5 rapidly deteriorated (GCS: 3) requiring emergency intubation. Upon arrival, blood pressure was found to be 200/100 mmHg and treatment with labetalol and hydrochlorothiazide (HCTZ) was started. A computerized tomography (CT) scan showed a massive left-brain hemorrhage associated with midline shifting and cerebral herniation.

The patient had a coronary stent in the anterior interventricular artery implanted 5 years before the accident. He had a full cardiovascular examination with myocardial scintigraphy two years after

the coronary stent insertion and no sign of dissection was observed at that time. He had never been diagnosed with genetic diseases linked to connective tissue disorders. The patient suffered of hypertension and was taking medications to treat it (HCTZ, a diuretic; Diovan; Norvasc); he also suffered from atherosclerosis and was taking atorvastatin (Lipitor; Pfizer) to reduce cholesterol levels. He was part of a research project involving the use of rivaroxaban (Xarelto; Bayer, an anticoagulant) to prevent progression of the coronary disease.

After the patient was declared brain dead with the heart still beating and under mechanical ventilation, diagnostic investigations were started to assess the patient for organ donation. A CT scan of the thorax and the abdomen revealed the presence of a chronic dissection of the aorta that extended helicoidally from the aortic root to the bifurcation of the aorta into the iliac arteries (Type A Stanford Classification), see Fig. 1(a and b). The ascending aorta was dilated at 7.2×7.7 cm in the anterior-posterior and lateral-lateral diameter. The coronary vessels, the celiac trunk vessels and the left renal artery were perfused through the true lumen of the aorta. The right renal artery was dissected at its origin with no perfusion of the right kidney. The liver and the left kidney were deemed suitable for transplantation and the family consented to their retrieval. The aorta was also retrieved for research purposes with the help of *Transplant Québec*, the official transplant coordination body for the province of Québec. The research was approved by the ethical committee of McGill University.

3. Mechanical characterization of the descending thoracic aorta with chronic dissection

The retrieved thoracic aorta was prepared removing the periaortic connective tissue and the arterial branches. It was then preserved in physiological saline solution at 4 °C and tested within 48 h from the time it was harvested from the heart-beating donor. The dissected aorta with respective dimensions is shown in Fig. 2 (a–c). The dissection progressed within the media. Fig. 2(c) shows the undulated surface of the false lumen, which originated from the dissection. Strips of 32×8 mm were cut from the descending portion and they went to a dissecting procedure to separate the three constitutive layers. The axial strips were cut from the true lumen (external part of the true lumen, where the three layers were intact). The circumferential strips had the intima and the dissected media from the wall shared between the true and false lumina, while the adventitia was taken from the exterior wall of the false lumen, as indicated in Fig. 2(c). The thickness of the layers was increased by severe remodeling that has happened due to the chronic dissection. Most probably the patient suffered from the dissection for a rather long time.

Quasi-static uniaxial tensile tests (0.032 mm/s) were performed after 9 preconditioning cycles identical in duration and extension to the final one; the experimental apparatus is described in Amabili et al. (2019a). The mechanical behavior of a layer of the aortic material is characterized by using the GOH model (Gasser et al., 2006); we assume an incompressible material with two families of collagen fibers that are symmetrically disposed relative to the tensile direction, which has no component in the radial direction. No additional families of fibers were considered, as instead was proposed by Sassani et al. (2015). The fibers have mean directions $\pm\beta$ with respect to the aortic circumferential direction, with a fiber dispersion described by the dispersion parameter $\kappa \in [0, 1/3]$, varying between zero for perfectly aligned fibers (transversely isotropic response), and 1/3 for equally distributed fibers (isotropic response). The strain-energy function W is (Gasser et al., 2006)

$$W = \frac{\mu}{2}(I_1 - 3) + \frac{\mu_1}{\mu_2} \left\{ \exp \left[\mu_2 (\kappa I_1 + (1 - 3\kappa) I_4 - 1)^2 \right] - 1 \right\}, \quad (1)$$

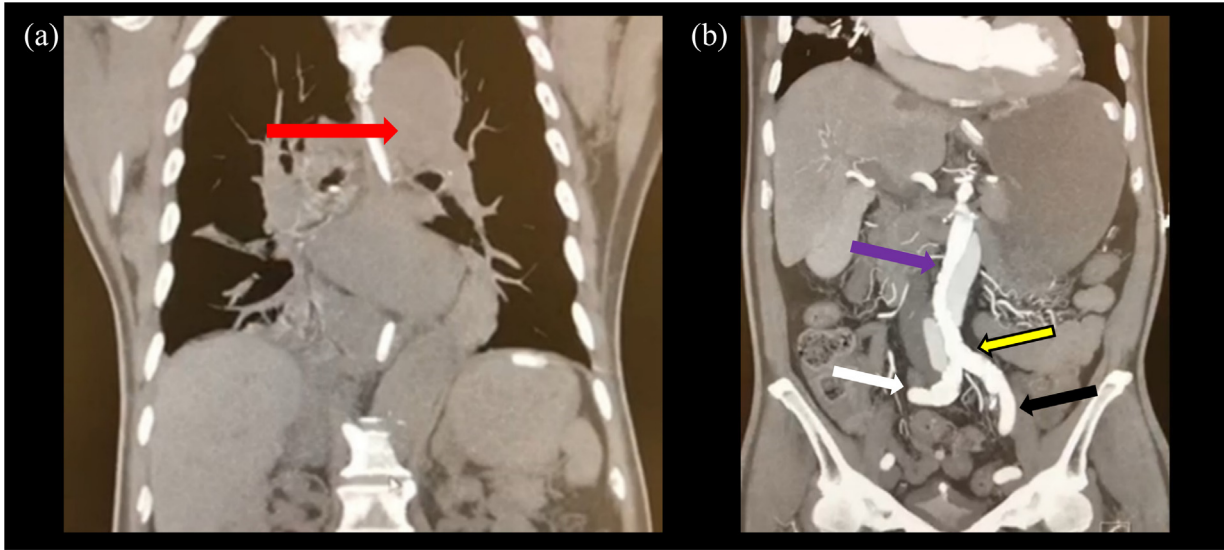


Fig. 1. (a) Coronal thoracic and (b) abdominal CT scan, displaying a chronic type A aortic dissection originating from the aortic root (red arrow) and extending to the aortic bifurcation (yellow arrow): (a) Aortic arch dissection (red arrow); (b) helicoidal path of the false lumen surrounding the true lumen (purple arrow) all through the abdominal portion of the aorta. The left (white arrow) and right (black arrow) iliac arteries are clearly visible. (For interpretation of the references to color in this figure legend, the reader is referred to the web version of this article.)

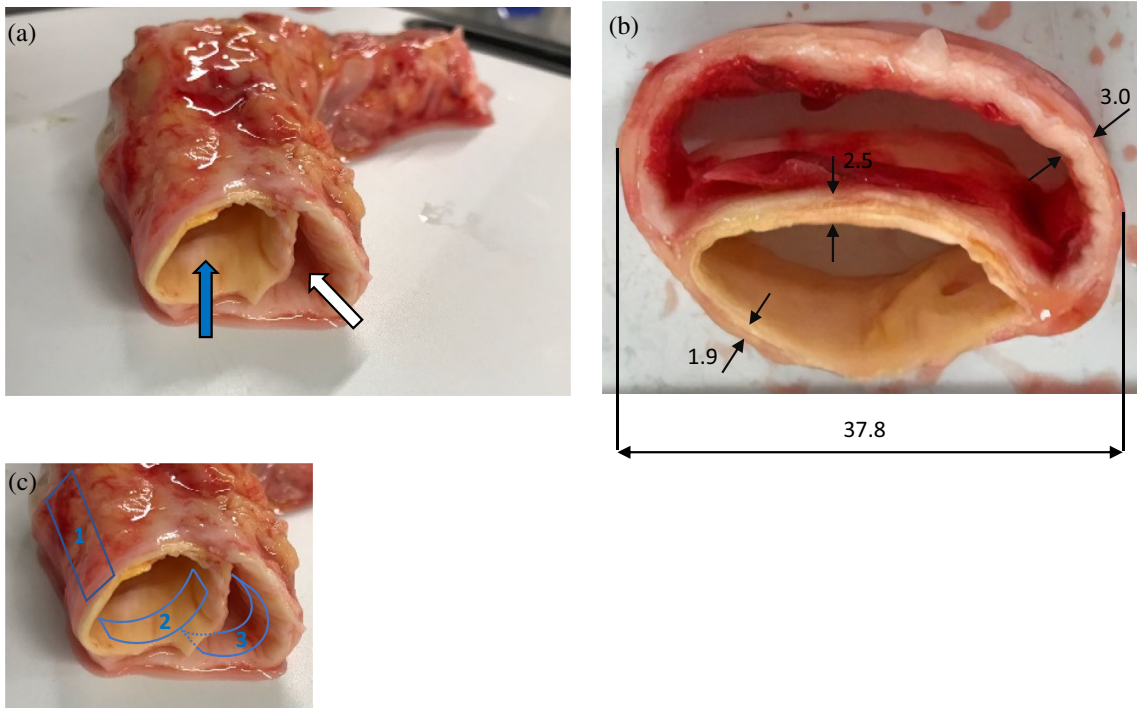


Fig. 2. (a) Retrieved thoracic aorta showing the true (blue arrow) and false lumen (white arrow); (b) dimensions (in mm) are drawn on a ring taken from the descending portion of the thoracic aorta – the true lumen is at the bottom; (c) position where the strips were cut out: 1 denotes the axial strip with the three layers, 2 the circumferential strip from the true lumen with the intima and the dissected media, and 3 denotes the circumferential strip from the false lumen with the adventitia (the dissected media from this strip was not tested). A few strips were cut in parallel in order to have spared samples for testing.

where the isotropic ground matrix is described by a neo-Hookean material (first term), with the first invariant I_1 of the right Cauchy-Green tensor \mathbf{C} (Amabili 2018), given by

$$I_1 = \text{tr}\mathbf{C} = 2(E_{xx} + E_{\theta\theta} + E_{rr}) + 3, \quad (2)$$

where $\text{tr}(\bullet)$ represents the trace of the tensor \bullet , and E_{xx} , $E_{\theta\theta}$ and E_{rr} are the components of the Green-Lagrange strain tensor in the axial, circumferential and radial direction, respectively. The radial Green-

Lagrange strain is then obtained by the incompressibility condition $\det\mathbf{C} \equiv 1$, i.e. in the absence of shear stresses

$$E_{rr} = \frac{1}{2(2E_{xx} + 1)(2E_{\theta\theta} + 1)} - \frac{1}{2}. \quad (3)$$

In Eq. (1), the pseudo-invariant I_4 takes on the following expression in the absence of shear (Amabili 2018), i.e.

$$I_4 = 1 + 2(E_{xx}\sin^2\beta + E_{\theta\theta}\cos^2\beta), \quad (4)$$

where μ and μ_1 are stress-like material parameters and μ_2 is a non-dimensional parameter. These parameters, together with the fiber angle β and the dispersion parameter κ were identified using a computer code based on genetic algorithms (Amabili et al., 2019a); hence the fiber angle and the dispersion parameter are here used as phenomenological parameters by fitting the material model (1) to the available experimental data. The invariants I_4 and I_6 contribute both in traction and compression since no fiber exclusion was implemented in this case. The two uniaxial tests of the same layer in axial and circumferential direction were fitted together to identify the model parameters. The equations and the objective function minimized by the code are given in Amabili et al. (2019a).

Uniaxial tensile tests were also performed at different frequencies of small-amplitude (50 μm) harmonic strain, superimposed to

an initial stretch λ , to characterize the nonlinear viscoelastic behavior of each layer of the dissected aorta by a custom-built apparatus (Amabili et al. 2019a, 2019b). 20 cycles were measured at each frequency: 10 were preconditioning and 10 were used for the actual measurement. Frequency was varied between 1 and 40 Hz, with a step of 2 Hz. The viscoelastic model, which was adopted for the aortic material, is the generalized Maxwell model with N_s elements composed of springs and dashpots (Amabili 2018), with the dynamic storage modulus E' and the loss tangent η given by

$$E'(\omega, \lambda) = E_\infty(\lambda) \left[1 + \sum_{m=1}^{N_s} \beta_m^\infty \frac{(\omega \tau_m)^2}{1 + (\omega \tau_m)^2} \right], \tag{5}$$

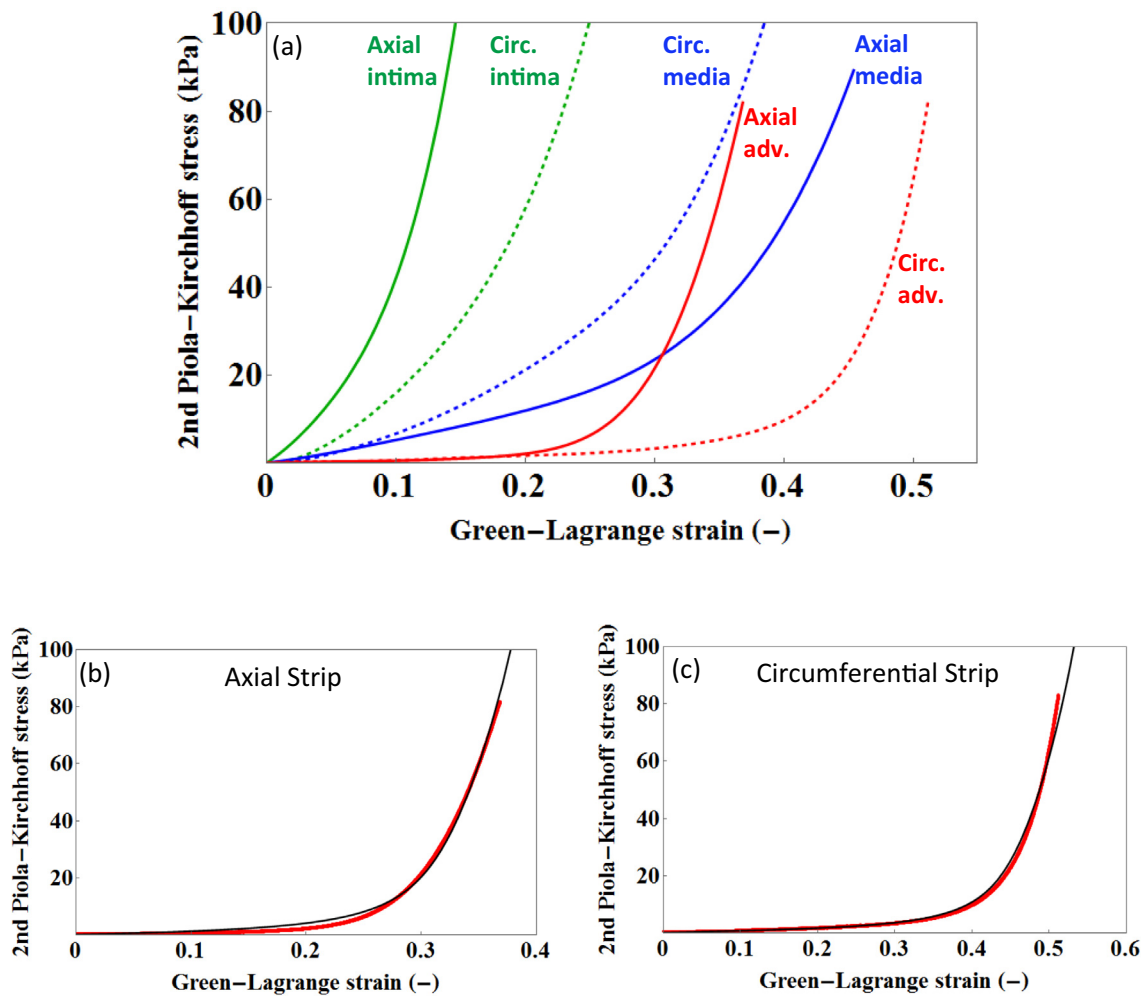


Fig. 3. Second Piola-Kirchhoff stress versus Green-Lagrange strain. (a) Experimental data from quasi-static uniaxial tensile tests (only loading curves are displayed) of the axial and circumferential strips from the intima, media and adventitia layers of the donor with chronic Type A dissected aorta. (b) Comparison of the model and the experimental data for the axial strip of adventitia; —, model; —, experiment. (c) Comparison of the model and the experimental data for the circumferential strip of adventitia; —, model; —, experiment.

Table 1
Identified quasi-static parameters for the GOH model and coefficient of determination R^2 . For the stiffness coefficient μ of the neo-Hookean term, the range of values determined from 12 healthy aortas (Amabili et al., 2019a) is provided within parentheses.

Layer	μ (kPa)	μ_1 (MPa)	μ_2	β ($^\circ$)	κ	R^2
Intima	58.5 (1.9–81.7)	14.0	54.2	42.3	0.0821	0.985
Media	11.8 (33.1–65.6)	0.416	13.2	46.4	0.0480	0.996
Adventitia	1.99 (6.3–38.2)	0.621	34.4	42.7	0.0193	0.995

$$\eta(\omega) = \frac{\sum_{m=1}^{N_S} \beta_m^\infty \frac{\omega \tau_m}{1+(\omega \tau_m)^2}}{1 + \sum_{m=1}^{N_S} \beta_m^\infty \frac{(\omega \tau_m)^2}{1+(\omega \tau_m)^2}} \quad (6)$$

where E_∞ is the static modulus (in Pa), $\beta_m^\infty > 0$ are non-dimensional material parameters, ω is the circular frequency (in rad/s) of strain and τ_m are material time constants (in s), while E_∞ is a function of the initial static stretch λ of the strip. Note that $E_\infty(\lambda)$ was obtained from the constitutive model (1). In particular, the storage modulus E' , as provided in (5), considers the parameter $E_\infty(\lambda)$, which makes E' dependent from the static stretch. The loss tangent η , as provided in (6), is instead independent of the initial static stretch.

4. Results and discussion

Fig. 3(a) shows the mechanical (static) behavior of the three layers (intima, media, adventitia) of the dissected aorta in axial and

circumferential directions. For small strains, the intima is the stiffest layer in both directions; it is followed by the dissected media in the circumferential direction, taken from the true lumen, and the media in the axial direction. The adventitia is initially the softest layer in both directions but becomes the stiffest in the higher stress region. The identified material parameters for the GOH constitutive model (1) and the coefficient of determination R^2 , assessing the accuracy of the fit, are summarized in Table 1. The parameters show a rather small dispersion parameter when compared to the study of Amabili et al. (2019a) in which twelve healthy aortas were investigated. In addition, the fiber angle β for the three layers is very similar ($\beta=42.3^\circ, 46.4^\circ$ and 42.7° for intima, media and adventitia, respectively), and close to 45° . The range of values obtained by Amabili et al. (2019a) for the material parameters are also summarized in Table 1. The comparison of data shows that the stiffness μ of the neo-Hookean term is three times smaller than the minimum value observed for the twelve healthy aortas for both media and adventitia. Some difference in the material properties can be

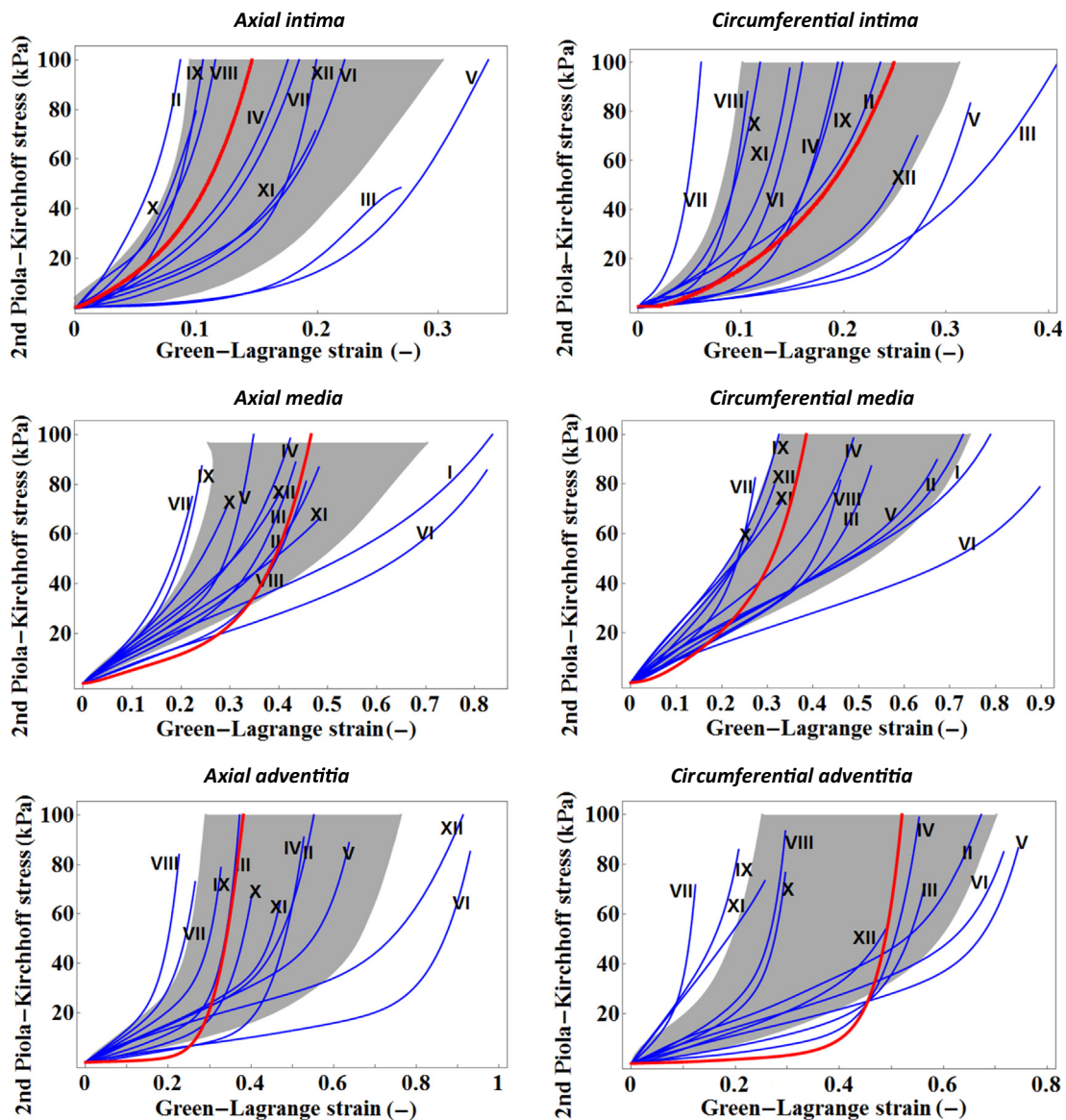


Fig. 4. Data from quasi-static uniaxial tensile tests (only loading curves are displayed) of the axial and circumferential strips from intima, media and adventitia of the donor with chronic dissected aorta (red curve). Blue curves, labeled with roman numbers, identify tests for healthy descending thoracic aortas as provided in Amabili et al. (2019a). Second Piola-Kirchhoff stress versus Green-Lagrange strain is shown. The gray area is within one standard deviation distance from the average curve obtained from all the healthy data for that specific layer and direction.

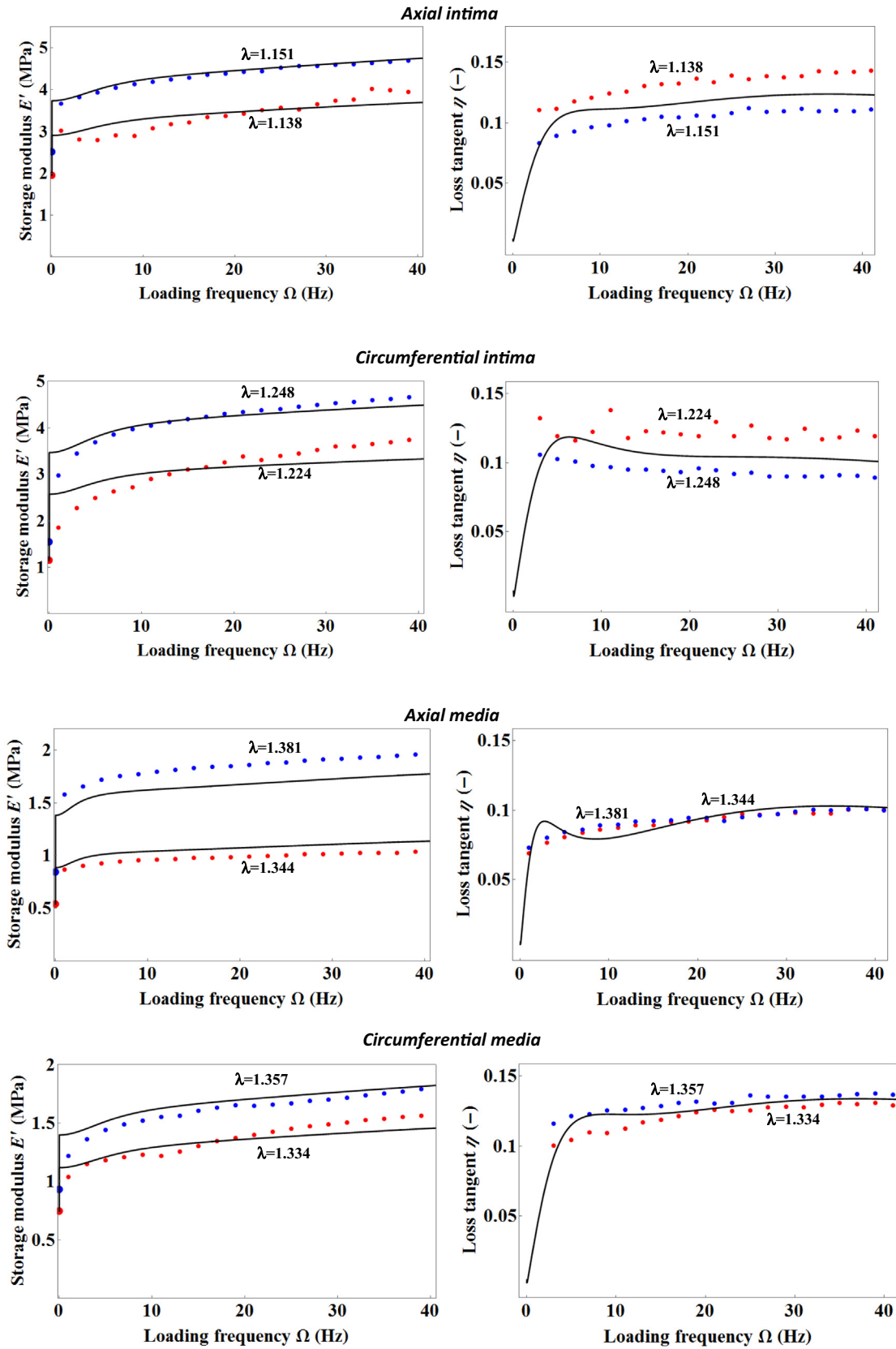


Fig. 5. Storage modulus E' and loss tangent η at two different initial stretches λ at the axial and circumferential strips from intima, media and adventitia of the dissected aorta versus loading frequency Ω (Hz). Generalized Maxwell model with $N_s = 5$. ● = experimental data for the smaller stretch; ● = experimental data for the larger stretch.

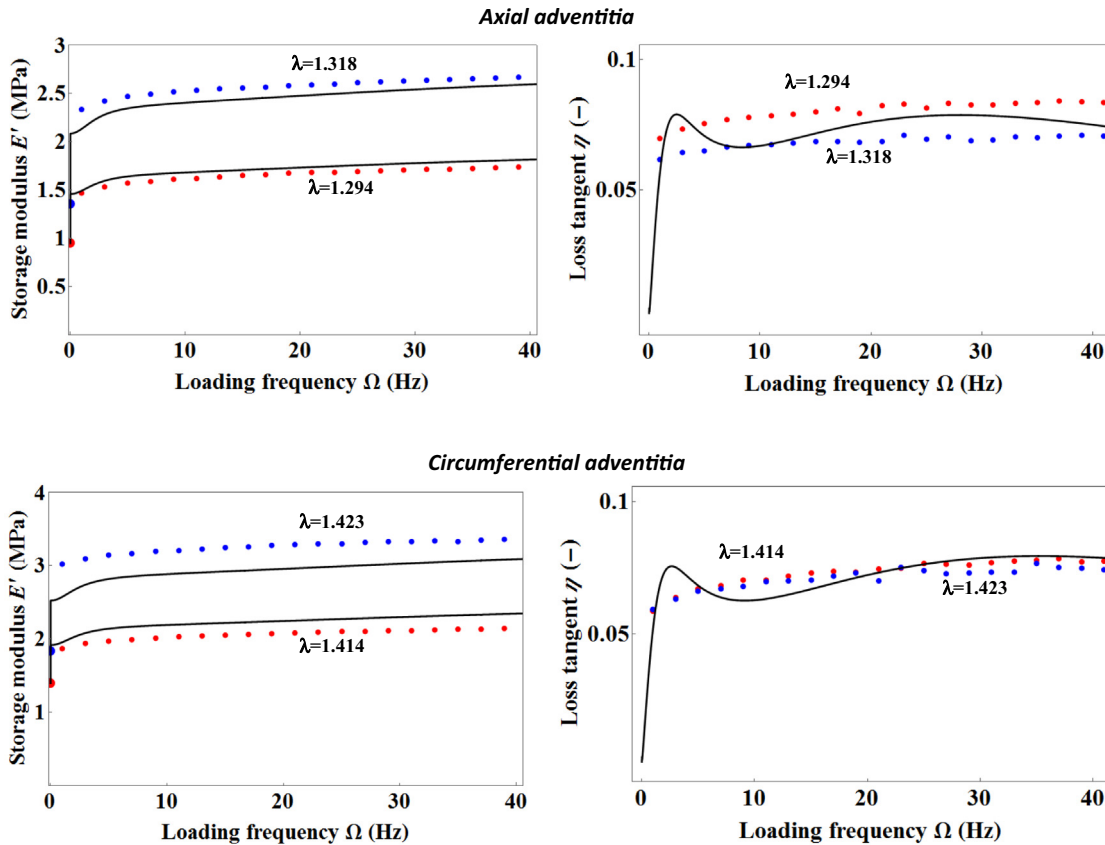


Fig. 5 (continued)

expected from strips taken at different locations. A satisfactory visual comparison of the material model and experiments for the adventitia are given in Fig. 3(b and c); they confirm the large value $R^2 = 0.995$ in Table 1 for this case.

A comparison of the (static) mechanical behavior of the six strips of the dissected aorta to healthy aortas tested by Amabili et al. (2019a) is carried out in Fig. 4. The stress–strain curves for the dissected intima lie approximately in the middle of the healthy intima curves, showing not much of a difference with respect to the mechanical response. On the other hand, the dissected media and adventitia present smaller stiffness at lower strains with respect to all the healthy cases, regaining a regular behavior for larger strains. It is not clear if this difference in the mechanical behavior is related to the strongly remodeled wall associated to the chronic dissection or if it was present before. The thicknesses of the three layers are: intima 0.2 mm; intact media in the axial strip 0.98 mm; adventitia in the false lumen 1.9 mm. While the intima and media have thicknesses comparable with those observed for healthy aortas (Amabili et al. 2019a), the adventitia has a thickness more than 2.5 times larger than the thickest adventitia observed in the same study. This is a solid indication of large remodeling of the

adventitia in the false lumen. The stress–strain relationship in the circumferential strip of the adventitia, which was taken from the false lumen, appeared to be most different among the studied regions compared to the healthy strips, as shown in Fig. 4.

The viscoelastic characterization of the dissected aorta is shown in Fig. 5, where both the storage modulus (dynamic stiffness) E' and the loss tangent (dissipation) η are provided for two different initial stretches λ of the six strips ($\Omega = \omega/2\pi$). The two levels of stretches in the dynamic tests are chosen to give a first Piola–Kirchhoff (engineering) stress of 50 and 100 kPa, respectively. Experimental data (dots) and the fitted generalized Maxwell model (curves) are shown. The viscoelastic material parameters are summarized in Table 2. Results show a sudden increase in the stiffness moving from static load (zero frequency) to dynamic load at 1 Hz, which is a characteristic of soft biological tissues. A relatively flat behavior is then observed in the remaining frequency range. The viscoelastic model in terms of the loss tangent, see Eq. (6), is independent of the initial stretch. This is well verified by the media and the circumferential adventitia in Fig. 5, while two distinct curves are experimentally observed for the intima and the axial adventitia. The two curves are roughly parallel, not far apart, and the low-

Table 2
Identified viscoelastic parameters for the generalized Maxwell model with $N_s = 5$. Ax = axial direction; Circ = circumferential direction; s = seconds.

Strip	β_1	β_2	β_3	β_4	β_5	τ_1 (s)	τ_2 (s)	τ_3 (s)	τ_4 (s)	τ_5 (s)
Intima Ax	0.403	0.252	0.137	0.173	0.177	0.003	0.026	1360	1570	1410
Intima Circ	0.464	0.482	0.224	0.345	0.674	0.003	0.028	1120	1300	1530
Media Ax	0.396	0.281	0.176	0.175	0.290	0.004	0.063	1240	1420	1470
Media Circ	0.451	0.294	0.146	0.147	0.205	0.003	0.026	1140	1260	1430
Adventitia Ax	0.264	0.226	0.112	0.279	0.147	0.005	0.070	1200	1490	1380
Adventitia Circ	0.242	0.194	0.153	0.100	0.119	0.004	0.065	1410	1320	1300

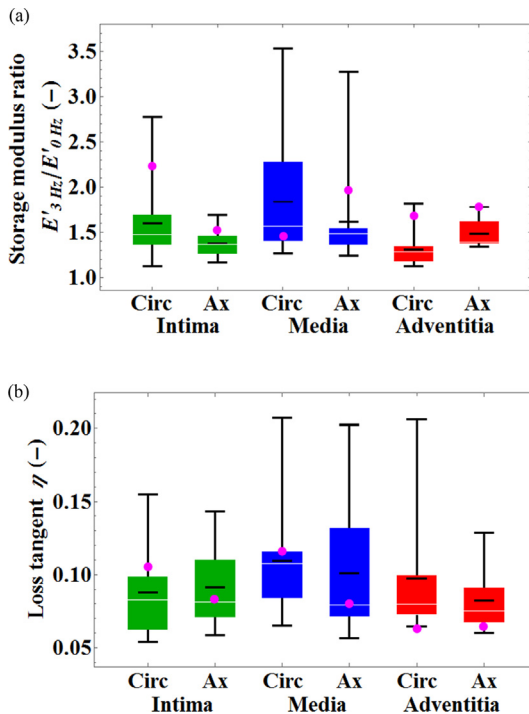


Fig. 6. Comparison of the viscoelastic behavior of the dissected aorta (magenta dot) to the statistical analysis of viscoelastic data from healthy descending thoracic aortas (Amabili et al., 2019a). Maximum, minimum, 1st quartile, 3rd quartile, average (black horizontal line inside the box) and median (white horizontal line in the box) are reported for the healthy aortas: (a) storage modulus ratio $E'_{3\text{Hz}}/E'_{0\text{Hz}}$; (b) loss tangent η at 3 Hz frequency; Ax = axial direction; Circ = circumferential direction.

est one is obtained for the largest stretch. This behavior shows the presence of nonlinear viscoelastic effects.

A comparison of the viscoelastic properties of the dissected aorta with the statistical analysis of data from twelve healthy aortas (Amabili et al., 2019a) is presented in Fig. 6. In particular, Fig. 6 (a) provides the storage modulus ratio $E'_{3\text{Hz}}/E'_{0\text{Hz}}$, which is related to the jump in stiffness from static to harmonic load at 3 Hz. Except for the media in the circumferential direction, the storage modulus ratio is outside the most probable region for healthy aortas, but still within the extreme values measured. Fig. 6(b) presents the loss tangent η at the frequency of 3 Hz. Both adventitia strips, in axial and circumferential directions, present rather low values for the loss tangent that are at the very limit of those measured by Amabili et al. (2019a).

The limitations of the study are (i) the number of locations from where the strips are taken, (ii) the absence of biaxial mechanical tests (no strain was measured orthogonally to the uniaxial extension direction), and (iii) the absence of a microscopy study to study the microstructure and statistical orientation of collagen fibers. It would be interesting to analyze the microarchitecture in a further study, even if it is very difficult to obtain tissue for a similar case.

5. Conclusion

A chronic Type A (Stanford) dissected aorta was retrieved from a heart-beating donor and its mechanical properties were studied. To our knowledge this is the first time that such quasi-static and dynamic studies were performed in chronic Type A aortic dissections. The aorta was dissected for the full length and it reached a diameter of 7.7 cm in the ascending part. The three layers of the aortic wall were separated and mechanically tested individually. Results of quasi-static uniaxial tensile tests show a physiological

(healthy) stiffness of the intima and some (mechanical) anomalies for the media and the adventitia that could be attributed to the strong remodeling of the wall associated to the chronic dissection.

In terms of the viscoelastic properties, the adventitia presented a larger relative increase of the dynamic stiffness to harmonic load at 3 Hz with respect to most of the healthy aortas reported in Amabili et al. (2019a). The loss factor of the adventitia was at the lower limit when compared with Amabili et al. (2019a). Results of dynamic tests reinforce the possibility of altered mechanical properties of the adventitia, which is a layer that largely thickened to allow the patient's survival to the chronic Type A aortic dissection. The role of remodeling after the acute phase of the dissection is the key factor for the patient survival in the chronic phase. Therefore, understanding the mechanical properties of the remodeled media and adventitia sheds new light on the knowledge of the progression of chronic Type A dissection.

Declaration of Competing Interest

The authors declare that they have no known competing financial interests or personal relationships that could have appeared to influence the work reported in this paper.

Acknowledgements

M.A. acknowledges the financial support of the NSERC Discovery Grant RGPIN-2018-06609, the Research Tool and Instrumentation grant of NSERC, and the Canada Research Chair program, while G.A.H. was partly supported by the Lead Project on "Mechanics, Modeling and Simulation of Aortic Dissection", granted by Graz University of Technology, Austria. The authors acknowledge the help of *Transplant Québec* that supplied the dissected aorta for the present research after obtaining specific consent.

References

- Ahmadzadeh, H., Rausch, M.K., Humphrey, J.D., 2019. Modeling lamellar disruption within the aortic wall using a particle-based approach. *Sci. Rep.* 9, 15320.
- Amabili, M., 2018. *Nonlinear Mechanics of Shells and Plates in Composite, Soft and Biological Materials*. Cambridge University Press, USA.
- Amabili, M., Balasubramanian, P., Bozzo, I., Breslavsky, I., Ferrari, G., 2019a. Layer-specific hyperelastic and viscoelastic characterization of human descending thoracic aortas. *J. Mech. Behav. Biomed. Mater.* 99, 27–46.
- Amabili, M., Balasubramanian, P., Breslavsky, I., 2019b. Anisotropic fractional viscoelastic constitutive models for human descending thoracic aortas. *J. Mech. Behav. Biomed. Mater.* 99, 186–197.
- Amabili, M., Balasubramanian, P., Bozzo, I., Breslavsky, I.D., Ferrari, G., Franchini, G., Giovanniello, F., Pogue, C., 2020. Nonlinear dynamics of human aortas for material characterization. *Phys. Rev. X* 10, 011015.
- Angouras, D.C., Kritharis, E.P., Sokolis, D.P., 2019. Regional distribution of delamination strength in ascending thoracic aortic aneurysms. *J. Mech. Behav. Biomed. Mater.* 98, 58–70.
- Bellini, C., Bersi, M.R., Caulk, A.W., Ferruzzi, J., Milewicz, D.M., Ramirez, F., Rifkin, D. B., Tellides, G., Yanagisawa, H., Humphrey, J.D., 2017. Comparison of 10 murine models reveals a distinct biomechanical phenotype in thoracic aortic aneurysms. *J. R. Soc. Interface* 14, 20161036.
- Emmott, A., Garcia, J., Chung, J., Lachapelle, K., El-Hamamsy, I., Mongrain, R., Cartier, R., Leask, R.L., 2016. Biomechanics of the ascending thoracic aorta: a clinical perspective on engineering data. *Can. J. Cardiol.* 32, 35–47.
- Erbel, R., Alfonso, F., Boileau, C., Dirsch, O., Eber, B., Haverich, A., Rakowski, H., Struyven, J., Radegran, K., Sechtem, U., Taylor, J., Zollikofer, Ch., Klein, W.W., Mulder, B., Providencia, L.A., 2001. Diagnosis and management of aortic dissection (Recommendations of the Task Force in Aortic Dissection, European Society of Cardiology). *Eur. Heart J.* 22, 1642–1681.
- Evangelista, A., Isselbacher, E.M., Bossone, E., Gleason, T.G., Eusanio, M.D., Sechtem, U., Ehrlich, M.P., Trimarchi, S., Braverman, A.C., Myrmet, T., Harris, K.M., Hutchinson, S., O'Gara, P., Suzuki, T., Nienaber, C.A., Eagle, K.A., 2018. Insights from the international registry of acute aortic dissection: A 20-year experience of collaborative clinical research (on behalf of the IRAD Investigators). *Circulation* 137, 1846–1860.
- Gasser, T.C., Ogden, R.W., Holzapfel, G.A., 2006. Hyperelastic modelling of arterial layers with distributed collagen fibre orientations. *J. R. Soc. Interface* 3, 15–35.
- Gültekin, O., Hager, S.P., Dal, H., Holzapfel, G.A., 2019. Computational modeling of progressive damage and rupture in fibrous biological tissues: application to aortic dissection. *Biomech. Model. Mechanobiol.* 18, 1607–1628.

- Guo, D.-C., Pannu, H., Tran-Fadulu, V., Papke, C.L., Yu, R.K., Avidan, N., Bourgeois, S., Estrera, A.L., Safi, H.J., Sparks, Amor, E.D., Ades, L., McConnell, V., Willoughby, C. E., Abuelo, D., Willing, M., Lewis, R.A., Kim, D.H., Scherer, S., Tung, P.P., Ahn, C., Buja, L.M., Raman, C.S., Shete, S.S., Milewicz, D.M., 2007. Mutations in smooth muscle alpha-actin (ACTA2) lead to thoracic aortic aneurysms and dissections. *Nat. Genet.* 39, 1488–1493.
- Hagan, P.G., Nienaber, C.A., Isselbacher, E.M., Bruckman, D., Karavite, D.J., Russman, P.L., Evangelista, A., Fattori, R., Suzuki, T., Oh, J.K., Moore, A.G., Malouf, J.F., Pape, L.A., Gaca, C., Sechtem, U., Lenferink, S., Deutsch, H.J., Diedrichs, H., Marcos y Robles, J., Llovet, A., Gilon, D., Das, S.K., Armstrong, W.F., Deeb, G.M., Eagle, K.A., 2000. The international registry of acute aortic dissection (IRAD): new insights into an old disease. *J. Am. Med. Assoc.* 283, 897–903.
- Manopoulos, C., Karathanasis, I., Kouerinis, I., Angouras, D.C., Lazaris, A., Tsangaris, S., Sokolis, D.P., 2018. Identification of regional/layer differences in failure properties and thickness as important biomechanical factors responsible for the initiation of aortic dissections. *J. Biomech.* 80, 102–110.
- Pal, S., Tsamis, A., Pasta, S., D'Amore, A., Gleason, T.G., Vorp, D.A., Maiti, S., 2014. A mechanistic model on the role of “radially-running” collagen fibers on dissection properties of human ascending thoracic aorta. *J. Biomech.* 47, 981–988.
- Pasta, S., Phillippi, J.A., Gleason, T.G., Vorp, D.A., 2012. Effect of aneurysm on the mechanical dissection properties of the human ascending thoracic aorta. *J. Thoracic Cardiovasc. Surg.* 143, 460–467.
- Pasta, S., Phillippi, J.A., Tsamis, A., D'Amore, A., Raffa, G.M., Pilato, M., Scardulla, C., Watkins, S.C., Wagner, W.R., Gleason, T.G., Vorp, D.A., 2016. Constitutive modeling of ascending thoracic aortic aneurysms using microstructural parameters. *Med. Eng. Phys.* 38, 121–130.
- Sassani, S.G., Tsangaris, S., Sokolis, D.P., 2015. Layer- and region-specific material characterization of ascending thoracic aortic aneurysms by microstructure-based models. *J. Biomech.* 48, 3757–3765.
- Sherifova, S., Holzapfel, G.A., 2019. Biomechanics of aortic wall failure with a focus on dissection and aneurysm: a review. *Acta Biomater.* 99, 1–17.
- Sommer, G., Gasser, T.C., Regitnig, P., Auer, M., Holzapfel, G.A., 2008. Dissection properties of the human aortic media: an experimental study. *J. Biomech. Eng.* 130, 021007.
- Sommer, G., Sherifova, S., Oberwalder, P.J., Dapunt, O.E., Ursomanno, P.A., DeAnda, A., Griffith, B.E., Holzapfel, G.A., 2016. Mechanical strength of aneurysmatic and dissected human thoracic aortas at different shear loading modes. *J. Biomech.* 49, 2374–2382.
- Thunes, J.R., Phillippi, J.A., Gleason, T.G., Vorp, D.A., Maiti, S., 2018. Structural modeling reveals microstructure-strength relationship for human ascending thoracic aorta. *J. Biomech.* 71, 84–93.
- Tong, J., Cheng, Y., Holzapfel, G.A., 2016. Mechanical assessment of arterial dissection in health and disease: Advancements and challenges. *J. Biomech.* 49, 2366–2373.